The dynamin-like GTPase Sey1p mediates homotypic ER fusion in *S. cerevisiae*

Kamran Anwar,[1] Robin W. Klemm,[3] Amanda Condon,[1] Katharina N. Severin,[3] Miao Zhang,[4,5] Rodolfo Ghirlando,[2] Junjie Hu,[4,5] Tom A. Rapoport,[3] and William A. Prinz[1]

[1]Laboratory of Molecular and Cell Biology and [2]Laboratory of Molecular Biology, National Institute of Diabetes and Digestive and Kidney Diseases, National Institutes of Health, Bethesda, MD 20892
[3]Howard Hughes Medical Institute, Department of Cell Biology, Harvard Medical School, Boston, MA 02115
[4]Department of Genetics and Cell Biology and [5]Tianjin Key Laboratory of Protein Sciences, College of Life Sciences, Nankai University, Tianjin 300071, China

The endoplasmic reticulum (ER) forms a network of tubules and sheets that requires homotypic membrane fusion to be maintained. In metazoans, this process is mediated by dynamin-like guanosine triphosphatases (GTPases) called atlastins (ATLs), which are also required to maintain ER morphology. Previous work suggested that the dynamin-like GTPase Sey1p was needed to maintain ER morphology in *Saccharomyces cerevisiae*. In this paper, we demonstrate that Sey1p, like ATLs, mediates homotypic ER fusion. The absence of Sey1p resulted in the ER undergoing delayed fusion in vivo and proteoliposomes containing purified Sey1p fused in a GTP-dependent manner in vitro. Sey1p could be partially replaced by ATL1 in vivo. Like ATL1, Sey1p underwent GTP-dependent dimerization. We found that the residual ER–ER fusion that occurred in cells lacking Sey1p required the ER SNARE Ufe1p. Collectively, our results show that Sey1p and its homologues function analogously to ATLs in mediating ER fusion. They also indicate that *S. cerevisiae* has an alternative fusion mechanism that requires ER SNAREs.

Introduction

The ER forms a highly dynamic network of sheets and tubules that extends throughout the cytoplasm. Homotypic ER fusion is required to maintain the ER as one continuous network. In metazoans, the fusion of ER membranes appears to be mediated by atlastins (ATLs; Orso et al., 2009), which are membrane-bound GTPases that belong to the dynamin family. The ATLs consist of a GTPase domain, a three-helix bundle, two closely spaced trans-membrane segments, and a C-terminal cytoplasmic tail (Moss et al., 2011). They localize to ER tubules and interact with proteins that are implicated in shaping ER tubules, the reticulons and DP1 (Hu et al., 2009). A role for the ATLs in ER fusion is supported by the observations that depletion of the ATLs or the overexpression of dominant-negative forms reduced the branching of ER tubules in tissue-culture cells. Furthermore, the addition of antibodies inhibited network formation in vitro, and proteoliposomes containing purified ATL underwent GTP-dependent fusion (Hu et al., 2009; Orso et al., 2009). Recent work suggested that fusion begins when two ATL molecules localized in different membranes bind GTP and form a dimer, thereby tethering the membranes together (Bian et al., 2011; Byrnes and Sondermann, 2011). After GTP hydrolysis and P_i release, the cytoplasmic domains of both ATL molecules undergo a major conformational change, pulling the apposing membranes together, resulting in their fusion. Fusion is also facilitated by the C-terminal tail, which follows the trans-membrane segments (Bian et al., 2011; Pendin et al., 2011). An alternative model of the role of GTP hydrolysis in ATL-mediated ER fusion has also been proposed (Morin-Leisk et al., 2011). Homotypic ER fusion by ATLs is distinct from fusion mediated by SNAREs (Wickner and Schekman, 2008). Here, three t-SNARE proteins in one membrane and a v-SNARE partner in another membrane zipper up to form a four-helix bundle, thereby forcing the fusion of the membranes. Subsequently, the helix bundle is disassembled by the NSF ATPase to allow the next round of fusion. Thus, in contrast to the ATL-mediated process, fusion, by itself, is independent of nucleotide hydrolysis.

K. Anwar and R.W. Klemm contributed equally to this paper.

Correspondence to William A. Prinz: wprinz@helix.nih.gov

Abbreviations used in this paper: ATL, atlastin; BME, 2-mercaptoethanol; DDM, dodecylmaltoside; GSH, glutathione; SC, synthetic complete; ss, signal sequence.

The Rockefeller University Press $30.00
J. Cell Biol. Vol. 197 No. 2 209–217
www.jcb.org/cgi/doi/10.1083/jcb.201111115

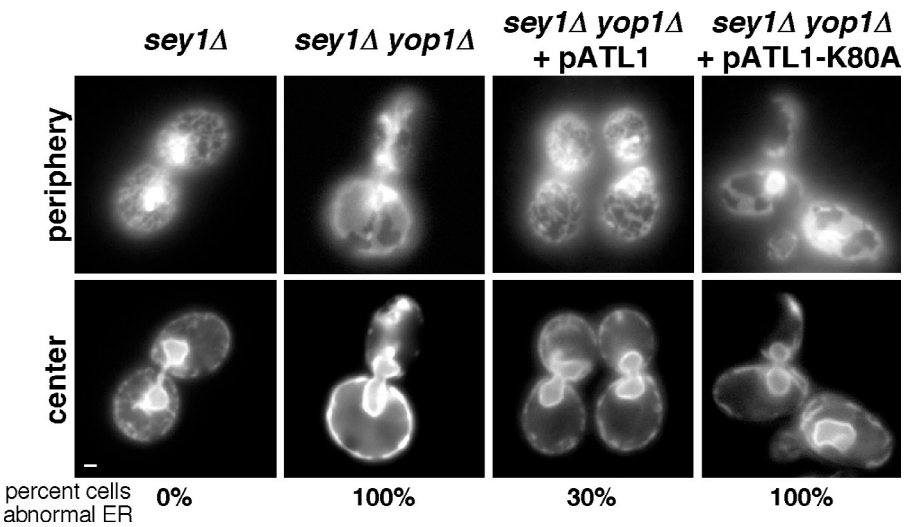

Figure 1. **ATL1 can functionally replace Sey1p in yeast.** Cells with the indicated genotypes expressing Sec63-GFP were visualized live, focusing on either the center plane or the periphery of the cells. Some cells also contained a plasmid encoding ATL1 or ATL1-K80A, a mutant defective in GTP-binding. Bar, 1 µm.

Many organisms, including yeast and plants, lack ATL homologues, raising the question of how they manage to fuse ER tubules into a network. However, these species have an analogous GTPase, called Sey1p in *Saccharomyces cerevisiae* and RHD3 in *Arabidopsis thaliana*. No organism seems to have both ATL and Sey1p homologues. Like ATL, Sey1p consists of a dynamin-like GTPase with characteristic signature motifs, a helical bundle domain (which is significantly longer than that of ATL), two closely spaced trans-membrane segments, and a C-terminal tail. Sey1p localizes to the tubular ER and interacts physically with the tubule-shaping proteins Rtn1p and Yop1p, which are homologues of the reticulons and DP1, respectively (Hu et al., 2009). Sey1p also interacts genetically with Yop1p (hence the name synthetic enhancer of Yop1p; Brands and Ho, 2002). We previously showed that deletion of *SEY1* alone had no obvious ER morphology defect, but deletion of both *SEY1* and *YOP1* or *SEY1* and *RTN1* resulted in the conversion of the tubular, cortical ER into sheets (Hu et al., 2009). Because cells missing only *YOP1* or *RTN1* have normal ER structure, the finding that cells missing Sey1p and either Rtn1p or Yop1 have abnormal ER morphology indicates that Sey1p plays a role in shaping the ER. Mutations in the plant ATL homologue RHD3 cause ER morphology defects similar to those seen with ATL mutants (Zheng et al., 2004; Yuen et al., 2005; Chen et al., 2011; Stefano et al., 2012). Despite these similarities, it was not clear whether Sey1p mediated ER fusion, particularly because there is little sequence similarity between Sey1p and ATLs, raising the question of whether Sey1p is truly a functional orthologue of the ATLs. Here, we show that Sey1p plays a role in homotypic ER fusion and can mediate GTP-dependent fusion of liposomes. Furthermore, we demonstrate that yeast contains a Sey1p-independent fusion mechanism that requires the ER SNARE Ufe1p.

Results and discussion

To determine whether Sey1p and human ATL1 have similar functions, we tested whether human ATL1 can replace Sey1p in *S. cerevisiae*. We have previously shown that cells missing the ER-shaping proteins Yop1p and Sey1p have abnormal ER morphology: they have a significant reduction in ER tubules and an increased amount of sheets (Fig. 1; Hu et al., 2009). The tubular ER network can be restored in a *sey1Δ yop1Δ* mutant by expressing wild-type Sey1p from a plasmid but not with a Sey1p mutant that is defective in GTP binding (Hu et al., 2009). To determine whether human ATL1 could replace Sey1p, we expressed ATL1 in *sey1Δ yop1Δ* cells that also express the ER-resident protein Sec63-GFP to visualize the ER. We found that wild-type ATL1 restored the ER tubular network in most *sey1Δ yop1Δ* cells, whereas a GTP-binding mutant of ATL1-K80A was inactive (Fig. 1). These data indicate that ATL1 can functionally replace Sey1p in maintaining ER morphology.

To investigate whether Sey1p functions in the fusion of ER tubules, we developed an in vivo assay that is similar to that used to study nuclear fusion (karyogamy) and mitochondrial fusion during the mating of yeast cells (Nunnari et al., 1997; Melloy et al., 2009; Tartakoff and Jaiswal, 2009). Haploid yeast cells expressing cytosolic GFP were mated with haploid cells expressing RFP in the ER lumen; RFP was targeted to the ER lumen by attaching a signal sequence (ss) to its N terminus and an ER retention signal to the C terminus (ss-RFP-HDEL). The GFP- and RFP-labeled cells were mixed, placed on an agarose pad, and imaged at 23°C every minute to follow the movement of the fluorescent proteins from one cell to the other. When cell fusion occurred, the cytosolic marker rapidly equilibrated between both cells, giving a starting point for the equilibration of the ER marker between the two cells. After two wild-type cells were mated, the ER marker began to equilibrate within a minute after cell fusion occurred (Fig. 2, a and b; and Video 1). Quantification of the fluorescence in both cells indicated that the decrease of the RFP signal in one cell can be accounted for by the increase of the RFP signal in the neighboring cell. Thus, the changes are not caused by newly synthesized ss-RFP-HDEL but rather by redistribution of protein from one cell to the other (Fig. 2 b). We found that with wild-type cells, the ER marker equilibrated ∼4 min after cell fusion (Fig. 2 e). When *sey1Δ* cells were mated with one another, the time necessary

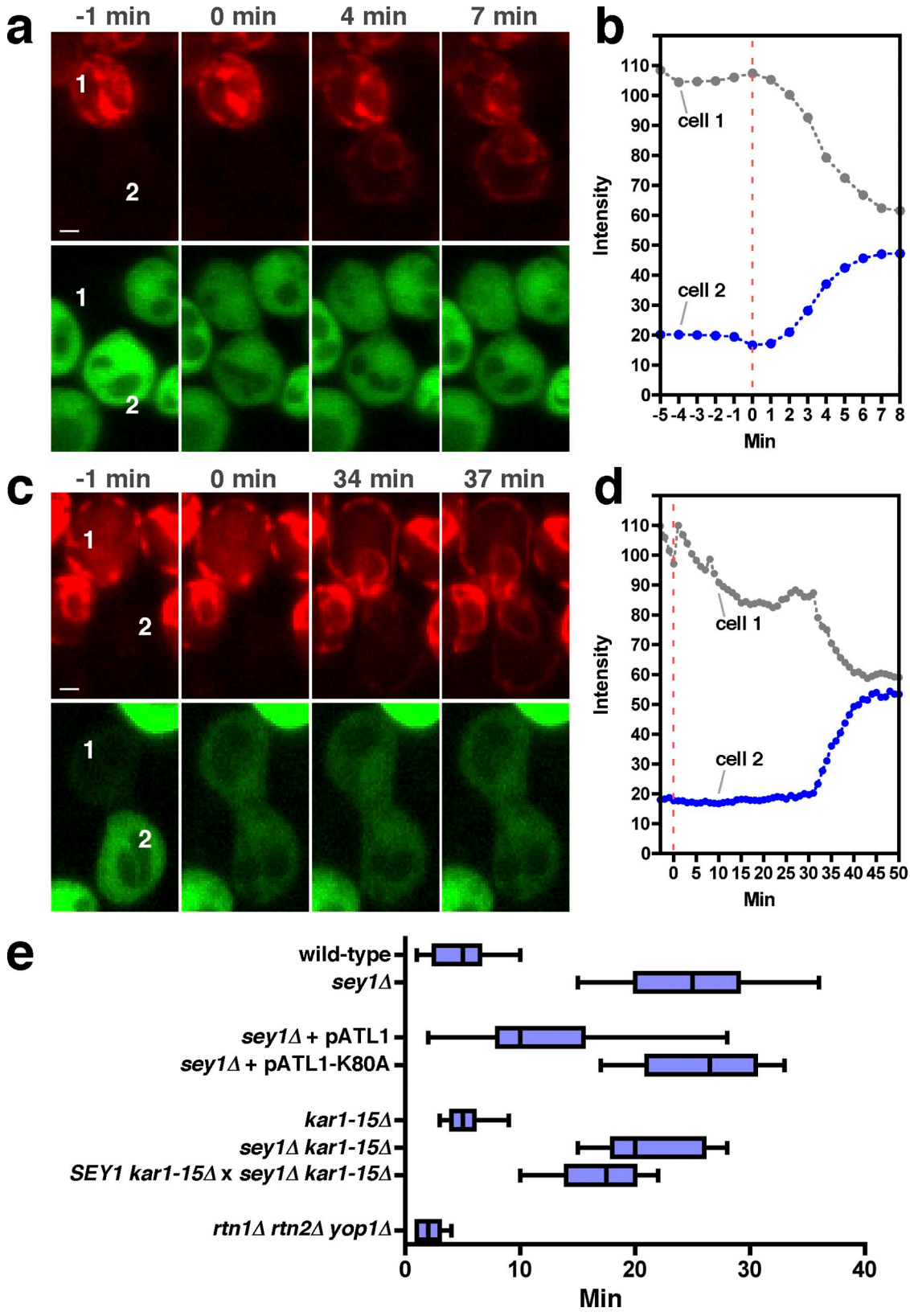

Figure 2. **ER–ER fusion is delayed in cells missing Sey1p.** (a) Wild-type cells of opposite mating types expressing either ss-RFP-HDEL or cytosolic GFP were mixed, placed on an agarose pad, and imaged at 1-min intervals. Selected images from the time-lapse video are shown. Time 0 is the first image taken after cell fusion, as indicated by GFP in both cells. The two cells of the analyzed mating pair are labeled 1 and 2. Bar, 1 μm. (b) Quantification of the RFP signal of cells 1 and 2 in a. (c) As in a, except that *sey1Δ* cells were used. (d) Quantification of the RFP signal of cells 1 and 2 in c. (e) A box and whiskers plot of the amount of time between cell fusion and ER fusion during mating. Top and bottom ends of the boxes represent the 75th and 25th percentiles, and whiskers indicate the maximum and minimum values. The median is depicted with a solid line (n = 15–25 from at least three independent experiments). Cells were mated at 23°C. Unless indicated, strains with identical genotypes were mated to each other.

for equilibration of the ER marker increased about sixfold (~25 min; Fig. 2, c–e; and Video 2).

One possibility is that the ER fusion that is ultimately observed is caused by nuclear envelope fusion. We tested this possibility by using the karyogamy mutant *kar1-15Δ*, in which the nuclei of the mating cells fail to fuse (Vallen et al., 1992). The results show that ER fusion in *kar1-15Δ* cells was indistinguishable from wild-type cells. Similarly, ER fusion was the same in *kar1-15Δ sey1Δ* and *sey1Δ* cells (Fig. 2 e). These results argue against a role of karyogamy in ER fusion. When *SEY1 kar1-15Δ* cells were mated with *sey1Δ kar1-15Δ* cells, ER fusion was as slow as when both cells lacked Sey1p (Fig. 2 e), indicating that Sey1p needs to be present in both cells to allow efficient ER fusion. Human ATL1 expressed in *sey1Δ* cells significantly improved ER fusion (Fig. 2 e); in many of the cells, the ER actually fused at a wild-type rate, but some cells showed delayed fusion. The cause of this variability is not known, but it may indicate that the expression levels of the ATL construct vary between cells or that ATL1 is only partially functional in yeast. However, a GTP-binding mutant of ATL1 (K80A) was inactive (Fig. 2 e), indicating that ATL activity is required for the rescue of the *sey1Δ* phenotype. The absence of the tubule-shaping proteins Rtn1p, Rtn2p, and Yop1p did not affect ER fusion (Fig. 2 e), indicating that aberrant ER morphology is not the reason for the observed fusion defects. Collectively, these data indicate that Sey1p indeed has a role in ER fusion and likely functions similarly to the ATLs.

The finding that ER fusion still occurs in *S. cerevisiae* in the absence of Sey1p indicates that another fusion mechanism must exist. Previous work has suggested that homotypic ER fusion requires Ufe1p, an essential ER SNARE (Patel et al., 1998). ER structure is disrupted in cells with a temperature-sensitive *ufe1-1* allele when they are shifted to a nonpermissive temperature (Prinz et al., 2000). We found a strong genetic interaction between *UFE1* and *SEY1*; although *ufe1-1* cells grow about as well as wild-type cells at a permissive temperature, *ufe1-1 sey1Δ* cells grow very poorly (Fig. 3 a). A similar genetic interaction was also found between *SEY1* and temperature-sensitive alleles of two other essential ER SNAREs, *USE1* and *SEC20* (Fig. S1, a and b). No genetic interaction was detected between the nonessential ER SNARE *SEC22* and *SEY1* (Fig. S1 c). We found that both Sey1p and Ufe1p are required for normal ER morphology. *ufe1-1 sey1Δ* cells have severely disrupted peripheral ER structure at a permissive temperature, whereas the single mutants have normal ER (Fig. 3 b; Hu et al., 2009).

We used the in vivo ER fusion assay to determine whether the rate of fusion decreases in *ufe1-1* cells. When *ufe1-1* cells were mated at permissive temperature (23°C), ER fusion occurred ~5 min after cell fusion (Fig. 3 c), similar to what was found for wild-type cells (Fig. 2 e). It was not possible to perform this assay with cells shifted to a nonpermissive temperature (37°C) immediately before mating because yeast will not mate at this temperature (Grote, 2010). Instead, we shifted cells to 32°C just before mating. At this temperature, *ufe1-1* strains were viable but grew much more slowly than wild-type cells (unpublished data), suggesting that Ufe1p function is substantially reduced at this temperature. When *ufe1-1* cells were mated at 32°C, ER fusion occurred a mean of ~10 min after cell fusion (Fig. 3 c), indicating that these cells have a modest fusion defect. At this temperature, cells missing only Sey1p fused their ER ~16 min after cell fusion (Fig. 3 c), somewhat faster than at 23°C (Fig. 2 e). However, when both Ufe1p and Sey1p were absent, fusion was dramatically affected; ER fusion occurred a mean of 37 min after cell fusion (Fig. 3 c). It is likely that ER fusion is not entirely abolished because some Ufe1p activity is retained at the semipermissive temperature used. Together, these findings suggest that both Ufe1p and Sey1p are involved in homotypic ER fusion in *S. cerevisiae*. Because ER fusion is less affected in cells missing only one of these two proteins than in the double mutant, Ufe1p and Sey1p may function in separate fusion pathways. If there are two pathways, overexpression of Sey1p might compensate for the decrease in the rate of homotypic ER fusion found in *ufe1-1* cells. We found that overexpression of Sey1p in *ufe1-1* cells at 32°C reduced the median time of ER–ER fusion in these cells from 10 to 6 min (Fig. 3 c), suggesting that Sey1p and Ufe1p indeed function in two separate pathways of ER–ER fusion.

It has been reported that the absence of ATLs in *Drosophila melanogaster* cells leads to fragmented ER, as determined by fluorescence loss in photobleaching experiments (Orso et al., 2009). This finding suggests that one of the primary functions of ATLs is to maintain the ER as one continuous network. We therefore tested whether the absence of Sey1p was also required to prevent ER fragmentation. Sec63p-GFP was expressed in *sey1Δ* cells, a portion of the ER was continuously bleached, and the cells were imaged over time (Fig. 3 d). The results show that the entire ER gradually loses fluorescence, indicating that the ER remains contiguous as in wild-type cells (Fig. 3 d). Similar results were obtained with *sey1Δ yop1Δ* cells (Fig. 3 d). Interestingly, *sey1Δ ufe1-1* cells also did not show fragmented ER, not even at the nonpermissive temperature (Fig. 3 d), at which ER morphology is severely disturbed (Fig. 3 b). Assuming that no ER fusion occurs in these cells, these findings suggest that there is little ER fission in yeast cells. It is also possible that there is a third fusion pathway in yeast that does not require Sey1p or Ufe1p.

To directly test whether Sey1p mediates ER fusion, we performed in vitro experiments. Full-length, codon-optimized Sey1p was expressed as a GST fusion protein in *Escherichia coli*. The protein was purified in the detergent dodecylmaltoside (DDM), the GST tag was removed, and the protein was reconstituted into proteoliposomes. The protein ran as a single band in SDS gels (Fig. 4 a) and was effectively reconstituted into vesicles, as demonstrated by flotation experiments (Fig. 4 a). Donor and acceptor proteoliposomes containing equal concentrations of Sey1p were used for the fusion assay (Fig. 4 b). The donor vesicles contained lipids labeled with two fluorophores at quenching concentrations, so that after fusion with unlabeled vesicles, the fluorophores were diluted, and quenching was reduced. The results show that Sey1p mediates fusion of the vesicles in a concentration-dependent manner (Fig. 4 c). No fusion was observed in the absence of magnesium ions (Fig. 4 c) or when GTP was replaced by GDP or by the nonhydrolyzable analogue GTPγS (Fig. 4 c). A GTP-binding mutant of Sey1p-K50A (Hu et al., 2009) did not support fusion (Fig. 4 d). Fusion was also reduced

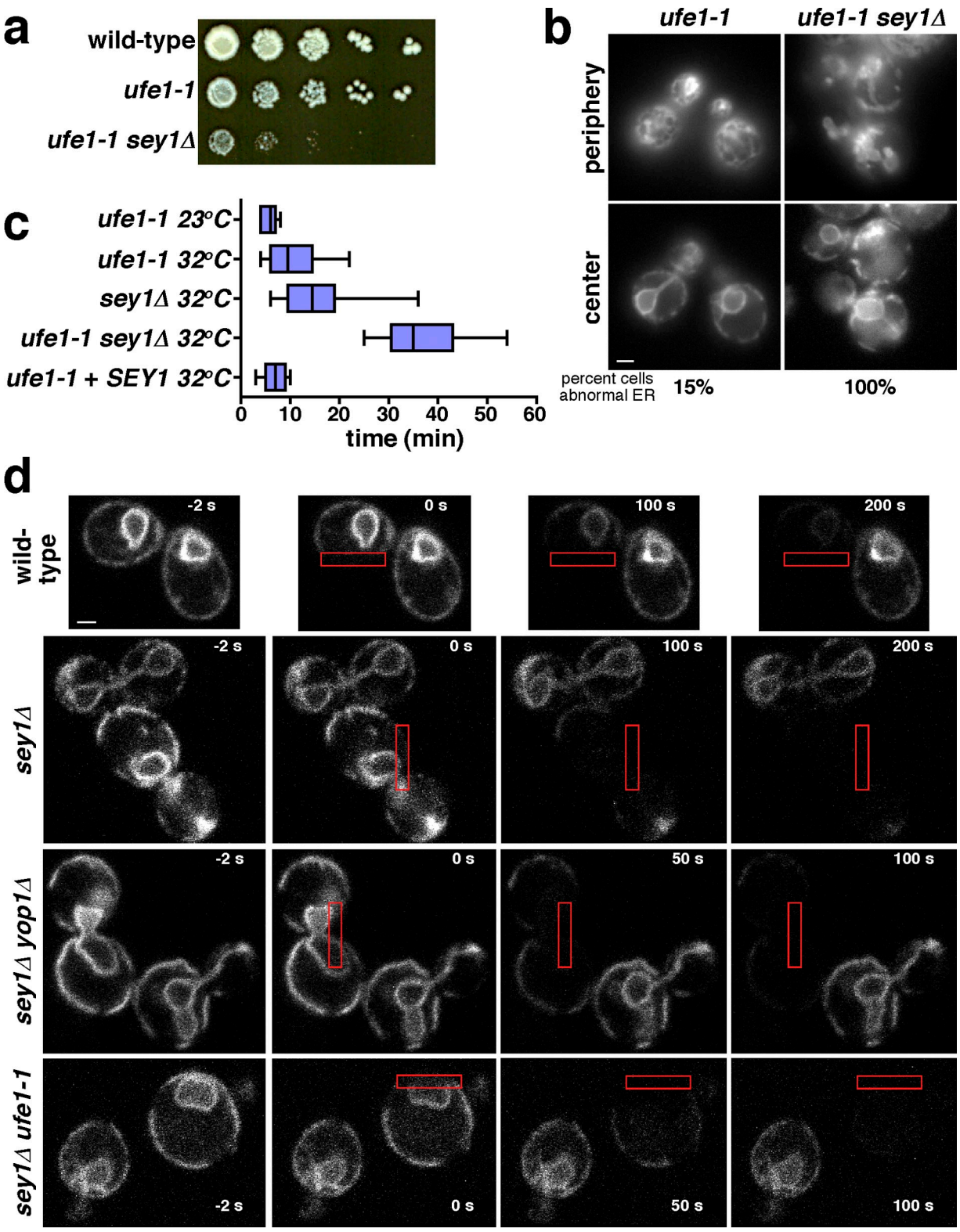

Figure 3. **Sey1p-independent ER–ER fusion requires the ER SNARE Ufe1p.** (a) Serial 10-fold dilutions of cells with the indicated genotypes were spotted onto YPD plates and incubated at 23°C for 5 d. (b) Cells with the indicated genotypes expressing Sec63-GFP were grown at 23°C and visualized live, focusing on either the center plane or the periphery of the cells. (c) A box and whiskers plot of the amount of time between cell fusion and ER fusion when cells with identical genotypes were mated with each other. Top and bottom ends of the boxes represent the 75th and 25th percentiles, and whiskers indicate the maximum and minimum values. The median is depicted with a solid line (n = 12–16 from at least three independent experiments). Cells were grown at 23°C and either mated at this temperature or shifted to 32°C immediately before mating. Where indicated (+ *SEY1*), the strains contained a plasmid that overexpressed Sey1p. (d) Strains expressing Sec63-GFP were visualized live in growth medium, and images were taken at 2-s intervals. Beginning at time 0, the area in the red rectangle was bleached every 2 s. Selected images from the time-lapse video are shown. All strains except *sey1Δ ufe1-1* were grown at 30°C. The *sey1Δ ufe1-1* cells were grown at 23°C and then shifted to 37°C for 30 min. Bars, 1 μm.

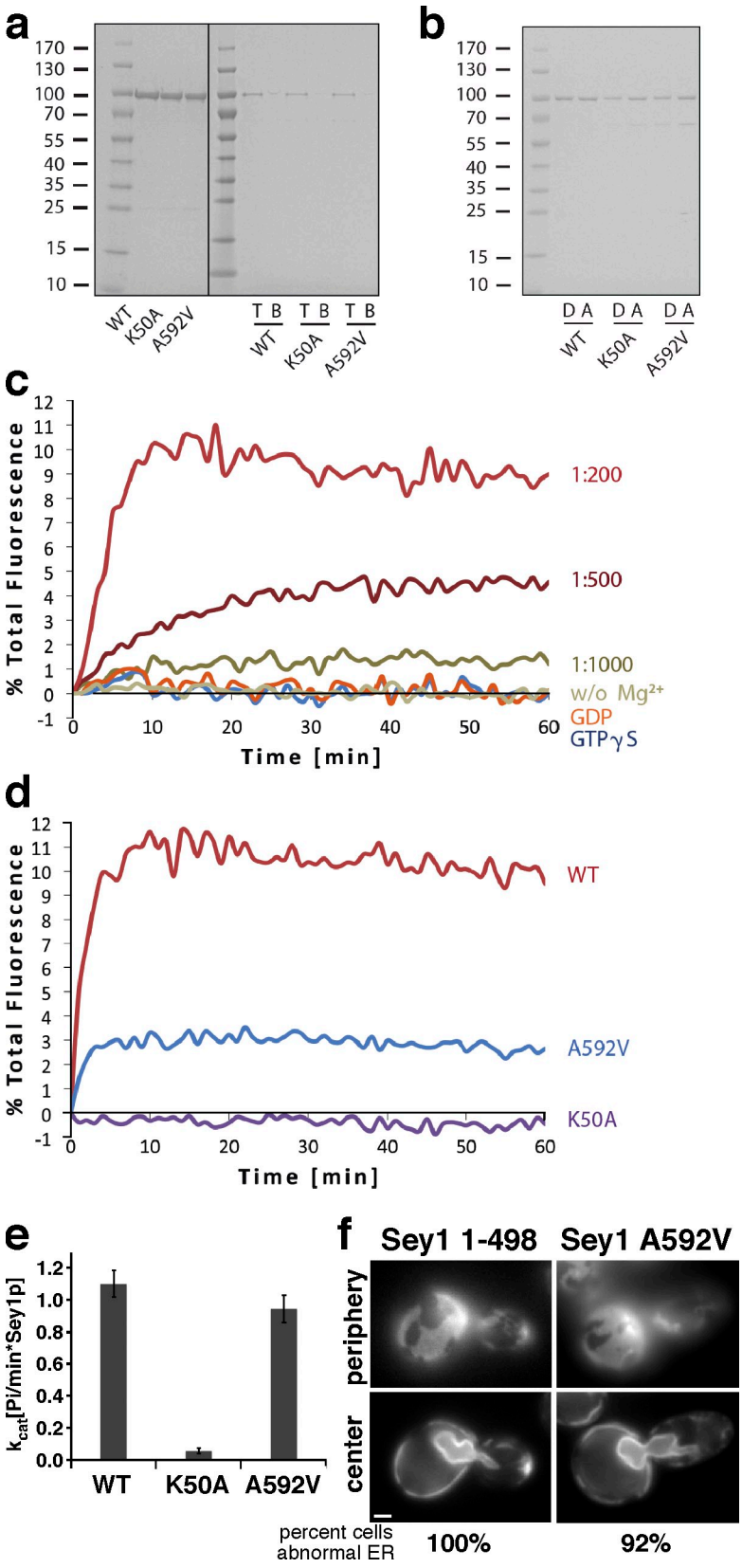

Figure 4. **Sey1p-mediated membrane fusion in vitro.** (a) Wild-type (WT) Sey1p or the indicated mutants were purified (left blot shows a Coomassie-stained SDS gel) and reconstituted into proteoliposomes. Flotation in a sucrose gradient (right) shows efficient reconstitution of the proteins (T, top fraction; B, bottom fraction). The black line indicates that intervening lanes have been spliced out. (b) Donor (D) and acceptor (A) proteoliposomes containing WT Sey1p or the indicated mutants were analyzed by SDS-PAGE and Coomassie staining. (c) WT Sey1p was reconstituted at the indicated protein to lipid ratios into proteoliposomes containing fluorescent lipids at quenching concentrations or unlabeled lipids (donor and acceptor vesicles, respectively). Donor and acceptor proteoliposomes were mixed at a ratio of 1:3 (600 µM of total lipid) and incubated for 10 min at 37°C before the addition of 1 mM GTP. The increase in fluorescence caused by lipid mixing was followed at 1-min intervals in a fluorescence plate reader. Control reactions were performed in the absence of Mg^{2+} or in the presence of GDP or GTPγS instead of GTP. (d) Fusion with WT Sey1p was compared with that of the indicated Sey1p mutants. Mutant Sey1K50A has a mutation in the phosphate-binding loop (P-loop) of the active site, and mutant A592V is analogous to one in a plant homologue that causes ER morphology defects. (e) GTPase activity of WT and the indicated Sey1p mutants. Error bars show means ± SD. (f) A *sey1Δ yop1Δ* strain expressing Sec63-GFP and plasmids encoding the indicated Sey1 mutants were visualized as in Fig. 1. Bar, 1 µm.

when a mutation was introduced into the helical bundle of Sey1p (A592V; Fig. 4 d); the analogous mutation in the plant protein RHD3 causes ER morphology defects (Wang et al., 1997). We confirmed that Sey1p-K50A has negligible GTPase activity, whereas Sey1p-A592V has near wild-type GTPase activity (Fig. 4 e and Fig. S2 a). In addition, expression of the A592V mutant of Sey1p, or of only the GTPase domain of Sey1p (Sey1 1–498), in a *sey1Δ yop1Δ* yeast strain did not restore the

tubular ER, indicating that the in vitro results are relevant to the situation in vivo (Fig. 4 f). Because we found that homotypic ER fusion in our in vivo fusion assay required that both cells express Sey1p (Fig. 2 e), we determined whether in vitro fusion had a similar requirement. No fusion was detected between proteoliposomes containing Sey1p and liposomes that did not contain Sey1p (Fig. S2 b). Interestingly, fusion was reduced but not completely abolished between proteoliposomes containing Sey1p and those with Sey1p-K50A; no fusion occurred when both proteoliposomes contained Sey1p-K50A. It may be that the low GTPase activity of Sey1p-K50A allows it to function, albeit inefficiently, when it interacts with wild-type Sey1p. Collectively, these results strongly support the notion that Sey1p mediates ER–ER fusion both in vitro and in cells.

To elucidate further the fusion mechanism, we investigated the oligomeric nature of Sey1p. We replaced the transmembrane domains of Sey1 (amino acids 681–727) with a 12–amino acid linker. The resulting protein, Sey1-ΔTM, was purified and subjected to sedimentation velocity analysis. Most of the protein ran as a monomer in the absence of nucleotide or in the presence of GDP but as a dimer in the presence of GDP and AlF_x as a mimic of the transition state of nucleotide hydrolysis (Fig. 5). These results are similar to those obtained for ATL (Bian et al., 2011; Byrnes and Sondermann, 2011).

Our in vivo and in vitro results strongly suggest that Sey1p functions in homotypic ER fusion in *S. cerevisiae*. It thus appears to be the functional orthologue of the ATLs in mammalian cells, for which in vitro data and ER morphology changes suggested a role in ER fusion. Now, the data for Sey1p provide strong evidence that the GTPases actually have a direct role in ER fusion in intact cells. As for the ATLs, the fusion reaction by Sey1p could begin with the GTP-dependent dimerization of GTPase domains sitting in apposing membranes (Bian et al., 2011). After GTP hydrolysis, a conformational change would occur, which pulls the membranes together and forces them to fuse. The predicted coiled-coil region of Sey1p is significantly longer than that of the ATLs, so the exact conformational change in Sey1p remains to be established.

In mammalian cells and in *Drosophila*, the ATLs may be the only ER fusogen, as their depletion or deletion results in long, unbranched ER tubules or fragmented ER tubules, respectively (Hu et al., 2009; Orso et al., 2009). The same may be true for Sey1p homologues in plants, as mutations in *A. thaliana* RHD3 cause drastic ER morphology defects (Zheng et al., 2004; Yuen et al., 2005; Chen et al., 2011; Stefano et al., 2012). However, in *S. cerevisiae*, there is clearly an additional fusion mechanism. The alternative pathway is not provided by nuclear envelope fusion, as demonstrated by the use of a karyogamy mutant, but is probably mediated by ER SNAREs. This hypothesis is supported by previous in vitro experiments (Patel et al., 1998) as well as by our finding that in vivo ER–ER fusion slows dramatically in *ufe1-1 sey1Δ* cells and by the strong negative genetic interactions of *SEY1* and *UFE1*. A similar strong negative interaction was also found between *SEY1* and genes encoding other essential ER SNAREs, *SEC22* and *USE1*. Therefore, ER SNAREs probably play a direct role in Sey1p-independent ER–ER fusion. Because SNAREs have essential functions in vesicular trafficking, it is difficult to evaluate the relative contributions of Sey1p- and SNARE-mediated homotypic ER fusion. Although our findings suggest that yeast has two different ER–ER fusion pathways, they do not exclude the possibility that, in intact cells, Sey1p and ER SNAREs could also cooperate in the same pathway.

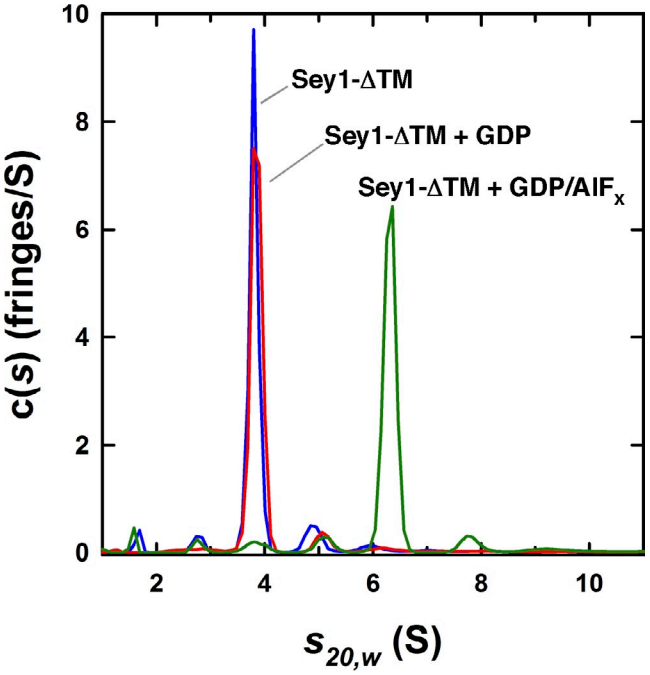

Figure 5. **Sey1p dimerizes in the presence of GDP AlF_x.** Analytical ultracentrifugation was used to calculate the c(s) distributions obtained for Sey1-ΔTM in the absence of nucleotide (blue) and in the presence of either 2 mM GDP (red) or 2 mM GDP, 2 mM $AlCl_3$, and 20 mM NaF (green). In the absence of nucleotide or presence of GDP, a molecular mass of 90 kD was determined for the major species at 3.85 S, consistent with a Sey1-ΔTM monomer (calculated molecular mass = 85.697 kD). In the presence of GDP AlF_x, the major species at 6.31 S had a molecular mass of 186 kD.

A surprising difference between our findings and work on *Drosophila* ATL (Orso et al., 2009) is that we found no ER fragmentation in *sey1Δ ufe1-1* cells at the nonpermissive temperature. One explanation could be that there is less ER fragmentation in yeast than in higher eukaryotes. In contrast to *S. cerevisiae*, in higher eukaryotes, the nuclear envelope breaks down, and there are dramatic alterations in ER morphology during mitosis, changes that may cause ER fragmentation. Thus, yeast may have little requirement for homotypic ER fusion during normal growth conditions.

Given that ER SNAREs associate and collaborate with COPI, the coat normally involved in Golgi–ER transport, it is interesting that a mutant in COPI causes ER morphology defects (Prinz et al., 2000). Recent results suggest that COPI plays a role in the generation of the cortical ER, independent from its role in retrograde vesicle transport (Lavieu et al., 2010). Thus, one may speculate that there is an ER SNARE- and COPI-dependent pathway of cortical ER fusion. The reason why this pathway may be sufficient to maintain ER morphology in yeast, but not in other organisms, could be that, in *S. cerevisiae*, the cortical ER represents a much larger percentage of the total ER (West et al., 2011).

Materials and methods

Strains

Strains used in this study are listed in Table S1. Strain RSY275 was obtained from R. Scheckman (University of California, Berkeley, Berkeley, CA), strain ACY85 was obtained from G. Fischer von Mollard (Universität Bielefeld, Bielefeld, Germany), and strains WPY804 and WPY805 were a gift from R. Rothstein (Columbia University, New York, NY).

Microscopy

Cells were imaged live in growth medium at room temperature using a microscope (BX61; Olympus), U Plan Apochromat 100×/1.35 NA lens, and a camera (Retiga EX; QImaging). IPLab version 3.6.3 software (Scanalytics) was used for image acquisition and analysis.

Fluorescence loss in photobleaching

Cells were imaged live in growth medium at room temperature using a laser-scanning inverted microscope (LSM 510 NLO; Carl Zeiss) using a Plan Neofluar 100×/1.3 NA oil objective with argon laser line of 488 nm (optical slices <1.1 µm). LSM 510 software version 3.2 (Carl Zeiss) was used for image acquisition and analysis. Magnification, laser power, and detector gains were identical across samples. Images were captured at 2-s intervals, and cells were photobleached every 2 s.

Analytical ultracentrifugation

Sey1 (Sey1-ΔTM) in which the two transmembrane domains of Sey1 (amino acids 681–727) were replaced with a 12–amino acid linker was used for analytical ultracentrifugation. A maltose-binding protein–Sey1-ΔTM fusion was expressed in *E. coli*, bound to amylose resin (New England Biolabs, Inc.), and eluted with 10 mM maltose. After overnight cleavage with Tobacco etch virus protease, Sey1-ΔTM was purified by size exclusion chromatography in 20 mM Tris-HCl, pH 8.0, 150 mM NaCl, 4 mM $MgCl_2$, 2 mM EGTA, and 2.5 mM 2-mercaptoethanol (BME; buffer A), in buffer A containing 2 mM GDP (buffer B), or in buffer B containing 2 mM $AlCl_3$ and 20 mM NaF (buffer C). Sedimentation velocity experiments were conducted at 20.0°C in an analytical ultracentrifuge (ProteomeLab XL-I; Beckman Coulter). 400 µl of 8.2-µM Sey1 GTPase each in buffers A, B, and C was loaded in the sample chamber of two-channel centerpiece cells, along with an equal volume of the matching buffer in the reference chamber. 45 scans, collected at a rotor speed of 50 krpm and 7.5-min intervals using the Rayleigh interference detection system (Beckman Coulter), were analyzed in SEDFIT 12.1b (Schuck, 2003) in terms of a continuous c(*s*) distribution of Lamm equation solutions covering an $s_{20,w}$ range of 1.0–15.0 S with a resolution of 140 and a confidence level of 0.68. We found that the Sey1 GTPase in buffer C had a slight excess of salt in the sample (corresponding to ∼0.8 fringes). To ensure that the best-fit frictional ratio required for the estimation of the molecular mass reflects only the protein contribution, data were analyzed in terms of a continuous c(*s*) distribution with one discrete component. The discrete component having a best-fit sedimentation coefficient of 0.6 S accounts for the contribution of the excess salt in the sample. We also found that the reference matching buffer B had a slightly larger refractive index (corresponding to ∼0.4 fringes) than that of the sample indicative of excess buffer components. To account for the signal offset arising from the unmatched sedimentation of solvent components, we modeled the contribution of the excess salt in the reference. This correction to the c(*s*) distribution is implemented in the buffer mismatch model of SEDFIT (Zhao et al., 2010). Excellent fits were obtained with root mean square deviation values ranging from 0.0030 to 0.0053 fringes. Solution densities (ρ) were measured at 20°C on a density meter (DE51; Mettler Toledo), and solution viscosities (η) were measured at 20°C using a rolling ball viscometer (AMVn; Anton Paar). The partial specific volume (*v*) of Sey1 GTPase was calculated in SEDNTERP 1.09 (Cole et al., 2008), and sedimentation coefficients (*s*) were corrected to $s_{20,w}$.

In vivo fusion assay

Cells of opposite mating types were grown to an OD (600 nm) of 0.1–0.4, mixed, and concentrated onto a filter (type HA, 25 mm, and 0.45-µm pore size; Millipore). The filters were placed cell side up on YPD (yeast extract/peptone/dextrose) plates and incubated at 30°C for ∼40–50 min. The cells were washed from the filters, pelleted for 2 min at 2,000 *g*, and resuspended in synthetic complete (SC) medium. 2 µl cell suspension was placed onto a 1-mm-thick pad made of 3% agarose and SC medium. The cells were covered with an 18-mm square coverslip, excess SC-agarose was cut off, and the edges were sealed with VALAP (equal parts Vaseline, lanolin, and paraffin). The cells were imaged using a laser-scanning microscope (LSM 5 Live; Carl Zeiss) and a Plan Apochromat 63×/1.4 NA oil differential interference contrast M27 objective with argon laser line at 488 and 532 nm (optical slices <1.7 µm). LSM 5 Live software version 4.2 SP1 was used for all image acquisitions and analysis. Magnification, laser transmission percentage, and detector gains were identical across samples. Images were captured at 60-s intervals with a scan time of 2.07 s.

Recombinant Sey1 production

Full-length *S. cerevisiae* SEY1 was PCR amplified from a codon-optimized, synthesized template (GenScript) using the oligonucleotides 5′-CTTCTGGATCCATGGCGGATCGTCCGGCC-3′ and 5′-CTGGACTCGAGTCATTTTTCTTTCTGTTCG-3′ as forward and reverse primers, respectively. The PCR product was digested with BamHI and XhoI and ligated into pGEX-4T-3 cut with the same enzymes. Recombinant wild-type and mutant GST-SEY1 was expressed in 4-liter cultures using BL21 cells and Luria broth medium containing 100 µg/ml ampicillin. Expression was started with 120 µM IPTG when cultures reached an OD_{600} of 0.8 and grown overnight at 16°C. The cells were harvested, resuspended in A200 (25 mM Hepes-KOH, pH 7.4, 200 mM KCl, 2 mM EDTA, 10% glycerol, and 2 mM BME), and lysed in a microfluidizer. The membranes were sedimented by centrifugation for 45 min at 4°C in a rotor (45 Ti; Beckman Coulter) at 40 krpm. The pellet was solubilized in A200 and 1.5% DDM (Anatrace) and separated from insoluble material by centrifugation as before. The extracts were incubated for 3 h with 1 ml glutathione (GSH)-Sepharose (GE Healthcare) and then washed with 50 ml A100 (25 mM Hepes-KOH, pH 7.4, 100 mM KCl, 1 mM EDTA, 10% glycerol, and 2 mM BME) containing 0.1% DDM. The protein was eluted from GSH-Sepharose with A100 containing 0.1% DDM and 10 mM of reduced GSH (Sigma-Aldrich). The fractions containing protein were pooled, and the GST tag was cleaved off by incubation with 25 U thrombin (GE Healthcare)/mg protein at 4°C overnight. GSH was removed using a desalting column (PD10; GE Healthcare), and the protein was separated from the GST moiety by incubation with 300 µl GSH-Sepharose. The purified protein was concentrated to 1 mg/ml and reconstituted into preformed liposomes.

Liposome production and protein reconstitution

For donor liposome production, POPC, DOPS, rhodamine-DPPE, and NBD-DPPE (Avanti Polar Lipids, Inc.) were mixed in a glass vial at a molar ratio of 82:15:1.5:1.5, respectively (10 mM of total lipid). For acceptor liposome formation, POPC, DOPS, and dansyl-DOPE were mixed at a molar ratio of 84:15:1.0. The chloroform was evaporated under a stream of N_2 gas, and the dried lipid film was rehydrated in A100. To produce large unilamellar vesicles, the multilamellar vesicles formed during the rehydration step were subjected to 10 freeze–thaw cycles using liquid N_2 and a water bath at room temperature. To form 100 nm–sized unilamellar liposomes, the large unilamellar vesicles were extruded 21 times through a polycarbonate filter with a pore size of 100 nm (Avestin). The total lipid concentration of donor and acceptor liposomes was determined by measuring NBD or dansyl fluorescence against a standard series, respectively (wavelengths: NBD, 460/538 nm and cutoff 515 nm; dansyl, 336/517 nm and cutoff 495 nm).

Protein reconstitution was performed by detergent-assisted insertions as previously described by Rigaud and Lévy (2003). Purified Sey1p in 0.1% DDM was mixed with preformed liposomes at the indicated molar ratios and an effective detergent to lipid ratio (R_{eff}) of 1.3 and incubated for 30 min at room temperature. R_{eff} is defined by the equation $R_{eff} = (D_{total} - D_{water})/[\text{total lipid}]$. D_{total} is the final detergent concentration; D_{water} is the critical micelle concentration of the detergent in the presence of lipid (0.3 for DDM; Rigaud and Lévy, 2003). Detergent was removed by four additions of SM-2 Bio-Beads (Bio-Rad Laboratories). Insoluble material was pelleted by centrifugation at 10 kg for 10 min and 4°C. Final proteoliposome concentration was determined by fluorescence as described for empty liposomes in the previous paragraph.

Proteoliposome flotation

The reconstitution efficiency was determined by flotation of proteoliposomes on a sucrose step gradient. 5 µl proteoliposomes (protein/lipid, 1:200) was mixed with 55 µl of 1.9-M sucrose (Sigma-Aldrich) and overlaid with 140 µl of 1.25-M sucrose and 40 µl of 0.25-M sucrose (all sucrose solutions are buffered by 25 mM Hepes-KOH, pH 7.4). After centrifugation at 55 krpm for 2 h and 4°C in a rotor using appropriate adaptors (TLS-55; Beckman Coulter), the gradient was fractionated into four 60-µl fractions and analyzed by SDS-PAGE stained with Coomassie.

In vitro fusion assay

In vitro membrane fusion was performed as previously described (Orso et al., 2009; Bian et al., 2011), except that donor and acceptor proteoliposomes were mixed at a molar ratio of 1:3. In brief, labeled donor proteoliposomes (150 µM of total lipid) were mixed with unlabeled acceptor proteoliposomes (450 µM of total lipid) in the presence of 5 mM Mg^{2+} and A100 in a total volume of 49 µl per reaction. The reaction mixture was transferred into a black polystyrene 96-well plate (Corning) and incubated at 37°C for 10 min. The fusion reaction was started by the addition of 1 mM GTP (final concentration). NBD fluorescence was measured at 1-min intervals. After 60 min, 10 µl of 2.5% DDM was added to determine total fluorescence in the sample. Fusion is expressed as the percentage of total fluorescence.

GTPase assay

GTPase activity was determined using the phosphate assay kit (EnzChek; Invitrogen) following the instructions of the manufacturer, except that the reaction buffer was replaced by A100. In brief, wild-type or mutant Sey1p was mixed with 0.5 mM GTP in a total volume of 200 µl per reaction. The samples were incubated for 15 min at 37°C, and the reaction was started by the addition of 5 mM Mg^{2+} (final concentration). Absorbance at 360 nm was measured at 1-min intervals for 30 min. The catalytic constant (k_{cat}) was determined using three different protein concentrations for wild type and each mutant and is expressed as P_i released per Sey1p molecule per minute ± standard.

Online supplemental material

Fig. S1 shows that there is a genetic interaction of *SEY1* with the gene encoding essential ER SNAREs other than Ufe1p. Fig. S2 shows that fusion efficiency is dependent on Sey1p GTPase activity. Videos 1 and 2 show ER fusion after mating wild-type (Video 1) or *sey1Δ* (Video 2) cells. Table S1 lists the strains used in this study. Online supplemental material is available at http://www.jcb.org/cgi/content/full/jcb.201111115/DC1.

We thank G. Fischer von Mollard, R. Rothstein, and R. Schekman for strains.

J. Hu is supported by the National Basic Research Program of China (973 Program; grant 2010CB833702). W.A. Prinz, K. Anwar, and A. Condon are supported by the Intramural Research Program of the National Institute of Diabetes and Digestive and Kidney Diseases. T.A. Rapoport is a Howard Hughes Medical Institute Investigator.

Submitted: 23 November 2011
Accepted: 15 March 2012

References

Bian, X., R.W. Klemm, T.Y. Liu, M. Zhang, S. Sun, X. Sui, X. Liu, T.A. Rapoport, and J. Hu. 2011. Structures of the atlastin GTPase provide insight into homotypic fusion of endoplasmic reticulum membranes. *Proc. Natl. Acad. Sci. USA*. 108:3976–3981. http://dx.doi.org/10.1073/pnas.1101643108

Brands, A., and T.H. Ho. 2002. Function of a plant stress-induced gene, HVA22. Synthetic enhancement screen with its yeast homolog reveals its role in vesicular traffic. *Plant Physiol.* 130:1121–1131. http://dx.doi.org/10.1104/pp.007716

Byrnes, L.J., and H. Sondermann. 2011. Structural basis for the nucleotide-dependent dimerization of the large G protein atlastin-1/SPG3A. *Proc. Natl. Acad. Sci. USA*. 108:2216–2221. http://dx.doi.org/10.1073/pnas.1012792108

Chen, J., G. Stefano, F. Brandizzi, and H. Zheng. 2011. *Arabidopsis* RHD3 mediates the generation of the tubular ER network and is required for Golgi distribution and motility in plant cells. *J. Cell Sci.* 124:2241–2252. http://dx.doi.org/10.1242/jcs.084624

Cole, J.L., J.W. Lary, T.P. Moody, and T.M. Laue. 2008. Analytical ultracentrifugation: sedimentation velocity and sedimentation equilibrium. *Methods Cell Biol.* 84:143–179. http://dx.doi.org/10.1016/S0091-679X(07)84006-4

Grote, E. 2010. Secretion is required for late events in the cell-fusion pathway of mating yeast. *J. Cell Sci.* 123:1902–1912. http://dx.doi.org/10.1242/jcs.066662

Hu, J., Y. Shibata, P.P. Zhu, C. Voss, N. Rismanchi, W.A. Prinz, T.A. Rapoport, and C. Blackstone. 2009. A class of dynamin-like GTPases involved in the generation of the tubular ER network. *Cell.* 138:549–561. http://dx.doi.org/10.1016/j.cell.2009.05.025

Lavieu, G., L. Orci, L. Shi, M. Geiling, M. Ravazzola, F. Wieland, P. Cosson, and J.E. Rothman. 2010. Induction of cortical endoplasmic reticulum by dimerization of a coatomer-binding peptide anchored to endoplasmic reticulum membranes. *Proc. Natl. Acad. Sci. USA*. 107:6876–6881. http://dx.doi.org/10.1073/pnas.1002536107

Melloy, P., S. Shen, E. White, and M.D. Rose. 2009. Distinct roles for key karyogamy proteins during yeast nuclear fusion. *Mol. Biol. Cell*. 20:3773–3782. http://dx.doi.org/10.1091/mbc.E09-02-0163

Morin-Leisk, J., S.G. Saini, X. Meng, A.M. Makhov, P. Zhang, and T.H. Lee. 2011. An intramolecular salt bridge drives the soluble domain of GTP-bound atlastin into the postfusion conformation. *J. Cell Biol.* 195:605–615. http://dx.doi.org/10.1083/jcb.201105006

Moss, T.J., A. Daga, and J.A. McNew. 2011. Fusing a lasting relationship between ER tubules. *Trends Cell Biol.* 21:416–423. http://dx.doi.org/10.1016/j.tcb.2011.03.009

Nunnari, J., W.F. Marshall, A. Straight, A. Murray, J.W. Sedat, and P. Walter. 1997. Mitochondrial transmission during mating in *Saccharomyces cerevisiae* is determined by mitochondrial fusion and fission and the intramitochondrial segregation of mitochondrial DNA. *Mol. Biol. Cell*. 8:1233–1242.

Orso, G., D. Pendin, S. Liu, J. Tosetto, T.J. Moss, J.E. Faust, M. Micaroni, A. Egorova, A. Martinuzzi, J.A. McNew, and A. Daga. 2009. Homotypic fusion of ER membranes requires the dynamin-like GTPase atlastin. *Nature*. 460:978–983. http://dx.doi.org/10.1038/nature08280

Patel, S.K., F.E. Indig, N. Olivieri, N.D. Levine, and M. Latterich. 1998. Organelle membrane fusion: a novel function for the syntaxin homolog Ufe1p in ER membrane fusion. *Cell*. 92:611–620. http://dx.doi.org/10.1016/S0092-8674(00)81129-0

Pendin, D., J. Tosetto, T.J. Moss, C. Andreazza, S. Moro, J.A. McNew, and A. Daga. 2011. GTP-dependent packing of a three-helix bundle is required for atlastin-mediated fusion. *Proc. Natl. Acad. Sci. USA*. 108:16283–16288. http://dx.doi.org/10.1073/pnas.1106421108

Prinz, W.A., L. Grzyb, M. Veenhuis, J.A. Kahana, P.A. Silver, and T.A. Rapoport. 2000. Mutants affecting the structure of the cortical endoplasmic reticulum in *Saccharomyces cerevisiae*. *J. Cell Biol.* 150:461–474. http://dx.doi.org/10.1083/jcb.150.3.461

Rigaud, J.L., and D. Lévy. 2003. Reconstitution of membrane proteins into liposomes. *Methods Enzymol.* 372:65–86. http://dx.doi.org/10.1016/S0076-6879(03)72004-7

Schuck, P. 2003. On the analysis of protein self-association by sedimentation velocity analytical ultracentrifugation. *Anal. Biochem.* 320:104–124. http://dx.doi.org/10.1016/S0003-2697(03)00289-6

Stefano, G., L. Renna, T. Moss, J.A. McNew, and F. Brandizzi. 2012. In *Arabidopsis*, the spatial and dynamic organization of the endoplasmic reticulum and Golgi apparatus is influenced by the integrity of the C-terminal domain of RHD3, a non-essential GTPase. *Plant J.* 69:957–966. http://dx.doi.org/10.1111/j.1365-313X.2011.04846.x

Tartakoff, A.M., and P. Jaiswal. 2009. Nuclear fusion and genome encounter during yeast zygote formation. *Mol. Biol. Cell*. 20:2932–2942. http://dx.doi.org/10.1091/mbc.E08-12-1193

Vallen, E.A., M.A. Hiller, T.Y. Scherson, and M.D. Rose. 1992. Separate domains of KAR1 mediate distinct functions in mitosis and nuclear fusion. *J. Cell Biol.* 117:1277–1287. http://dx.doi.org/10.1083/jcb.117.6.1277

Wang, H., S.K. Lockwood, M.F. Hoeltzel, and J.W. Schiefelbein. 1997. The ROOT HAIR DEFECTIVE3 gene encodes an evolutionarily conserved protein with GTP-binding motifs and is required for regulated cell enlargement in *Arabidopsis*. *Genes Dev.* 11:799–811. http://dx.doi.org/10.1101/gad.11.6.799

West, M., N. Zurek, A. Hoenger, and G.K. Voeltz. 2011. A 3D analysis of yeast ER structure reveals how ER domains are organized by membrane curvature. *J. Cell Biol.* 193:333–346. http://dx.doi.org/10.1083/jcb.201011039

Wickner, W., and R. Schekman. 2008. Membrane fusion. *Nat. Struct. Mol. Biol.* 15:658–664. http://dx.doi.org/10.1038/nsmb.1451

Yuen, C.Y., J.C. Sedbrook, R.M. Perrin, K.L. Carroll, and P.H. Masson. 2005. Loss-of-function mutations of ROOT HAIR DEFECTIVE3 suppress root waving, skewing, and epidermal cell file rotation in *Arabidopsis*. *Plant Physiol.* 138:701–714. http://dx.doi.org/10.1104/pp.105.059774

Zhao, H., P.H. Brown, A. Balbo, M. del C. Fernández-Alonso, N. Polishchuck, C. Chaudhry, M.L. Mayer, R. Ghirlando, and P. Schuck. 2010. Accounting for solvent signal offsets in the analysis of interferometric sedimentation velocity data. *Macromol. Biosci.* 10:736–745. http://dx.doi.org/10.1002/mabi.200900456

Zheng, H., L. Kunst, C. Hawes, and I. Moore. 2004. A GFP-based assay reveals a role for RHD3 in transport between the endoplasmic reticulum and Golgi apparatus. *Plant J.* 37:398–414. http://dx.doi.org/10.1046/j.1365-313X.2003.01969.x